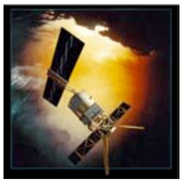

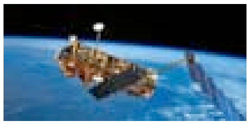

Satellite Remote Sensing
SIO 135/SIO 236

Lecture 7: Propagation, Dispersion and Scattering

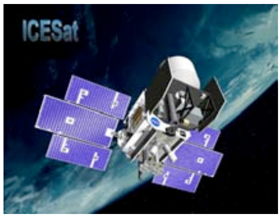

Helen Amanda Fricker

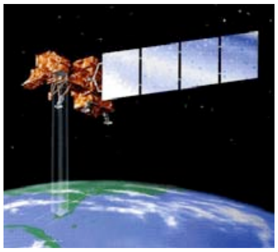

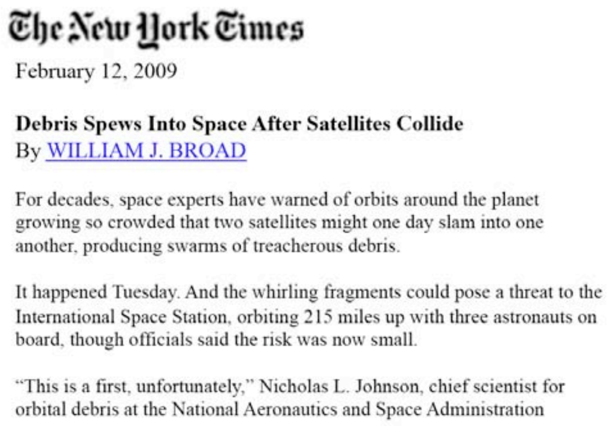

The New York Times

February 12, 2009

Debris Spews Into Space After Satellites Collide

By WILLIAM J. BROAD

For decades, space experts have warned of orbits around the planet growing so crowded that two satellites might one day slam into one another, producing swarms of treacherous debris.

It happened Tuesday. And the whirling fragments could pose a threat to the International Space Station, orbiting 215 miles up with three astronauts on board, though officials said the risk was now small.

"This is a first, unfortunately," Nicholas L. Johnson, chief scientist for orbital debris at the National Aeronautics and Space Administration

Iridium Coverage

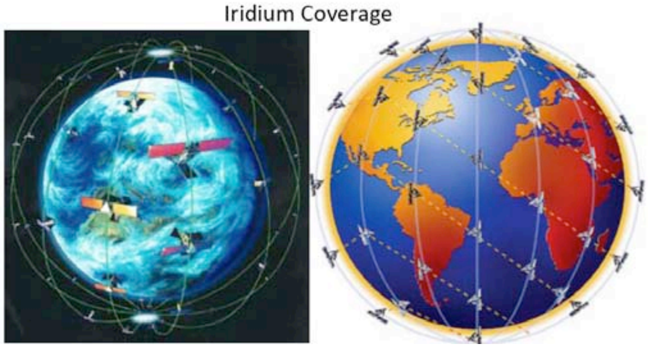

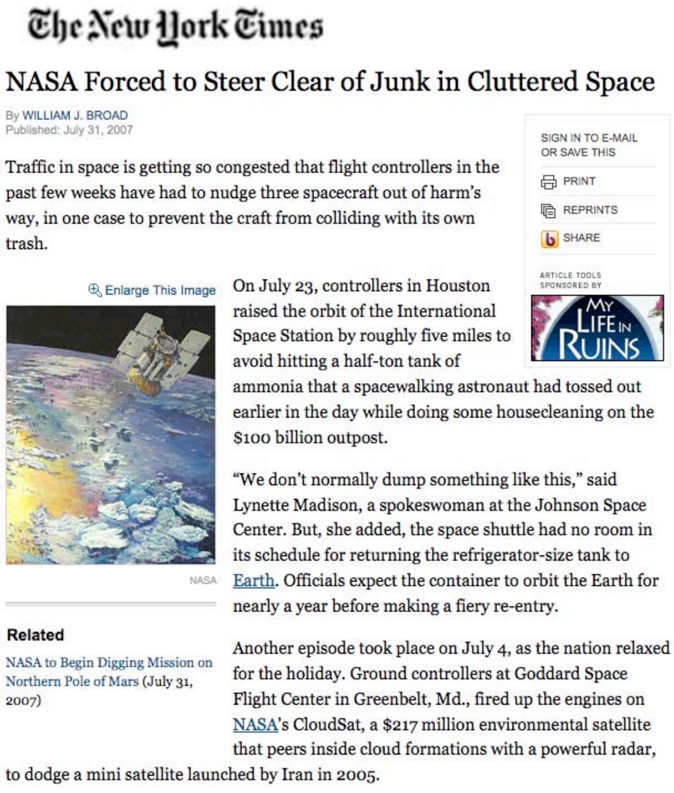

The New York Times

NASA Forced to Steer Clear of Junk in Cluttered Space

By WILLIAM J. BROAD
Published: July 31, 2007

Traffic in space is getting so congested that flight controllers in the past few weeks have had to nudge three spacecraft out of harm's way, in one case to prevent the craft from colliding with its own trash.

On July 23, controllers in Houston raised the orbit of the International Space Station by roughly five miles to avoid hitting a half-ton tank of ammonia that a spacewalking astronaut had tossed out earlier in the day while doing some housecleaning on the $100 billion outpost.

"We don't normally dump something like this," said Lynette Madison, a spokeswoman at the Johnson Space Center. But, she added, the space shuttle had no room in its schedule for returning the refrigerator-size tank to Earth. Officials expect the container to orbit the Earth for nearly a year before making a fiery re-entry.

Another episode took place on July 4, as the nation relaxed for the holiday. Ground controllers at Goddard Space Flight Center in Greenbelt, Md., fired up the engines on NASA's CloudSat, a $217 million environmental satellite that peers inside cloud formations with a powerful radar, to dodge a mini satellite launched by Iran in 2005.

Related

NASA to Begin Digging Mission on Northern Pole of Mars (July 31, 2007)

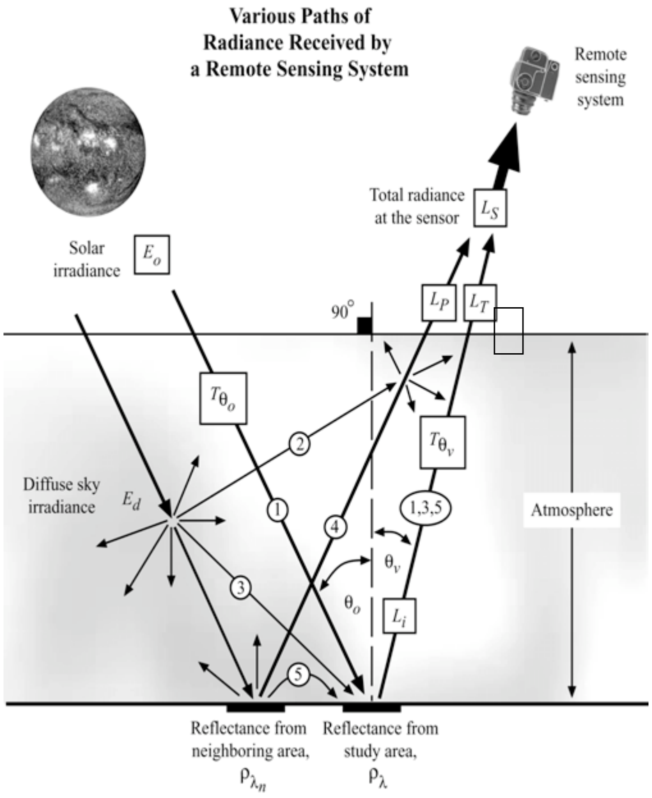

Energy-matter interactions

- atmosphere
- study region
- detector

Interactions under consideration

- Interaction of EMR with the atmosphere

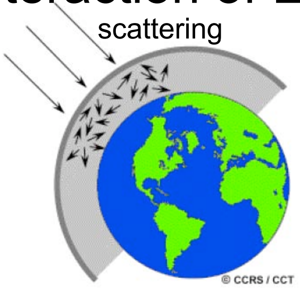

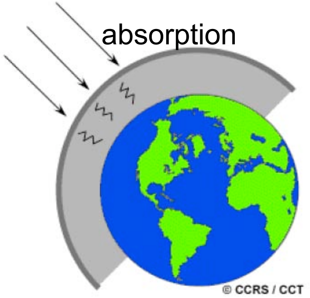

- Interaction of EMR with matter

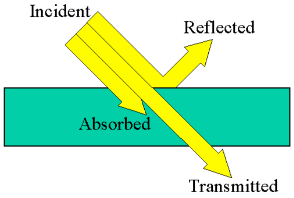

Interaction of EMR with the atmosphere

- EMR is **attenuated** by its passage through the atmosphere via scattering and absorption

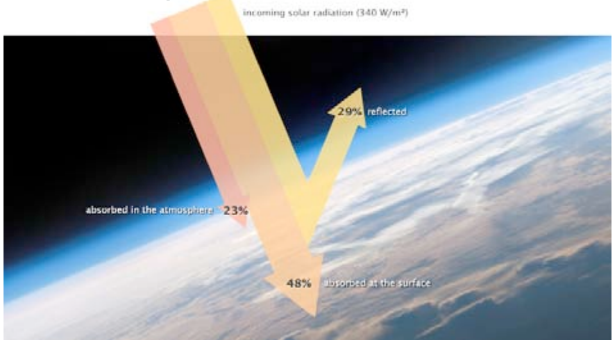

- Scattering -- differs from reflection in that the direction associated with scattering is unpredictable, whereas the direction of reflection is predictable.
- Wavelength dependent
- Decreases with increase in radiation wavelength
- Three types: Rayleigh, Mie & non selective scattering

Atmospheric Layers and Constituents

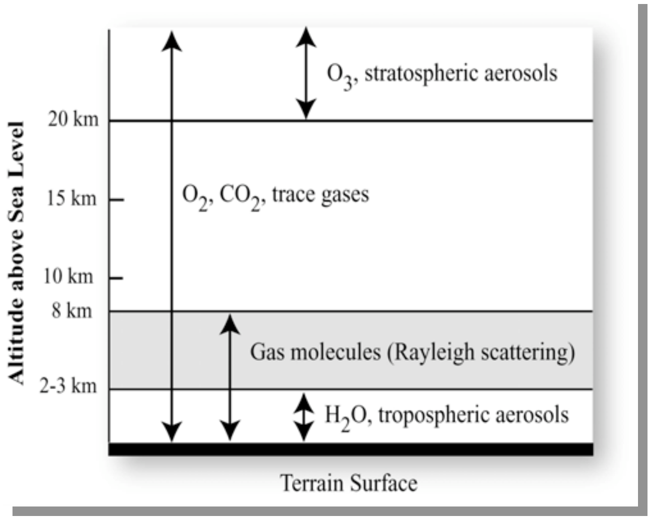

Jensen 2005

Major subdivisions of the atmosphere and the types of molecules and aerosols found in each layer.

Atmospheric Scattering

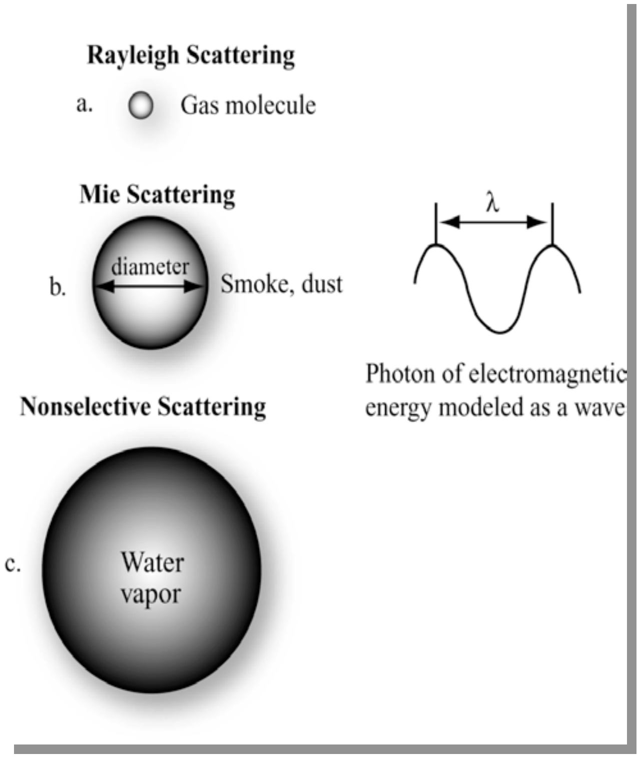

Type of scattering is function of:

1) the wavelength of the incident radiant energy, and

2) the size of the gas molecule, dust particle, and/or water vapor droplet encountered.

Jensen 2005

Rayleigh scattering

- Rayleigh scattering is molecular scattering and occurs when the diameter of the molecules and particles are many times smaller than the wavelength of the incident EMR

- Primarily caused by air particles i.e. O_2 and N_2 molecules

- All scattering is accomplished through absorption and re-emission of radiation by atoms or molecules in the manner described in the discussion on radiation from atomic structures. It is impossible to predict the direction in which a specific atom or molecule will emit a photon, hence scattering.

- The energy required to excite an atom is associated with short-wavelength, high frequency radiation. The amount of scattering is inversely related to the fourth power of the radiation's wavelength (λ^{-4}).

Rayleigh scattering

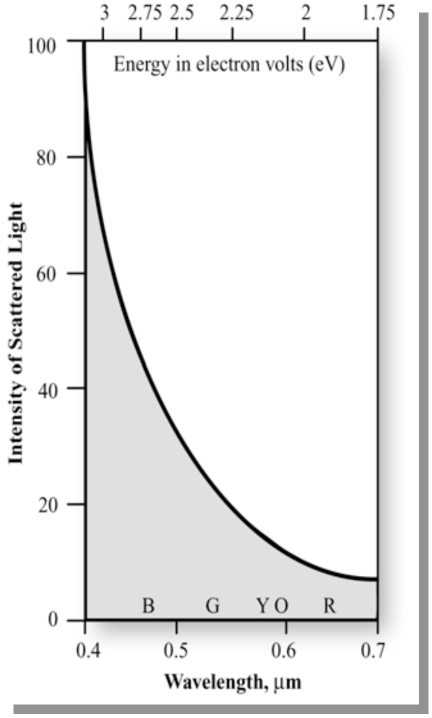

The intensity of Rayleigh scattering varies inversely with the fourth power of the wavelength (λ^{-4}).

So blue light (0.4 µm) is scattered 16 times more than near-infrared light (0.8 µm).

Jensen
2005

Rayleigh scattering

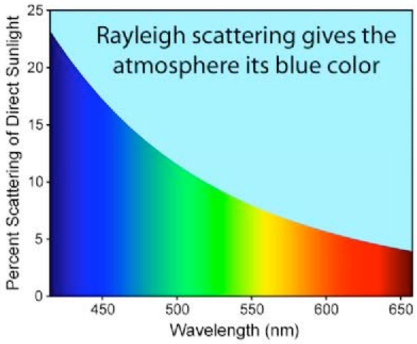

- Responsible for the blue sky. The short wavelengths (violet/blue) are more efficiently scattered than the longer wavelengths (orange/red). Blue sky is a result of the preferential scattering of the short wavelength light.

- Responsible for red sunsets. Since the atmosphere is a thin shell of gravitationally bound gas surrounding the solid Earth, sunlight must pass through a longer slant path of air at sunset/sunrise than at noon. Short wavelengths (violet/blue) are scattered even more during their longer path through the air, what we see when we look toward the Sun is the residue - the long wavelengths of sunlight that are hardly scattered (orange/red).

Rayleigh scattering

The approximate amount of Rayleigh scattering in the atmosphere in optical wavelengths (0.4 – 0.7 μm) may be computed using the Rayleigh scattering cross-section (τ_m) algorithm:

$$\tau_m = \frac{8\pi^3\left(n^2-1\right)^2}{\left(3N^2\lambda^4\right)}$$

where n = refractive index, N = number of air molecules per unit volume, and λ = wavelength.

Mie scattering

- Mie scattering takes place when there are essentially spherical particles present in the atmosphere with diameters approximately equal to the wavelength of radiation.

- For visible light, water vapor, dust, and other particles ranging from a few tenths of a micrometer to several micrometers in diameter are the main scattering agents. The amount of scatter is greater than Rayleigh scatter and the wavelengths scattered are longer.

- Pollution also contributes to beautiful sunsets and sunrises. The greater the amount of smoke and dust particles in the atmospheric column, the more violet and blue light will be scattered away and only the longer orange and red wavelength light will reach our eyes.

Non-selective scattering

- Non-selective scattering is produced when there are particles in the low atmosphere several times the diameter of the radiation being transmitted. This type of scattering is non-selective, i.e. all wavelengths of light are scattered, not just blue, green, or red. Thus, water droplets, which make up clouds and fog banks, scatter all wavelengths of visible light equally well, causing the cloud to appear white

- Scattering can severely reduce the information content of remotely sensed data to the point that the imagery looses contrast and it is difficult to differentiate one object from another.

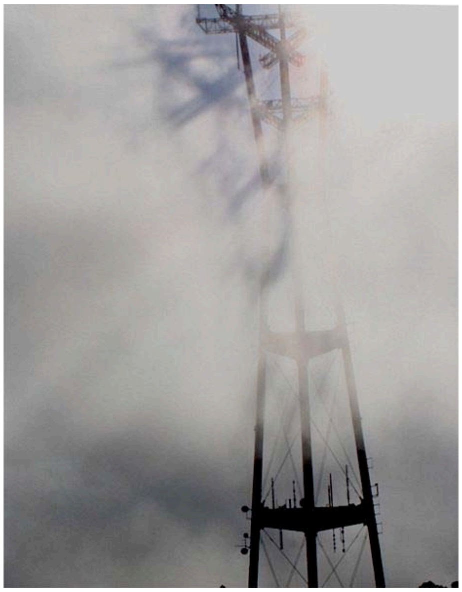

Absorption of EMR by atmosphere

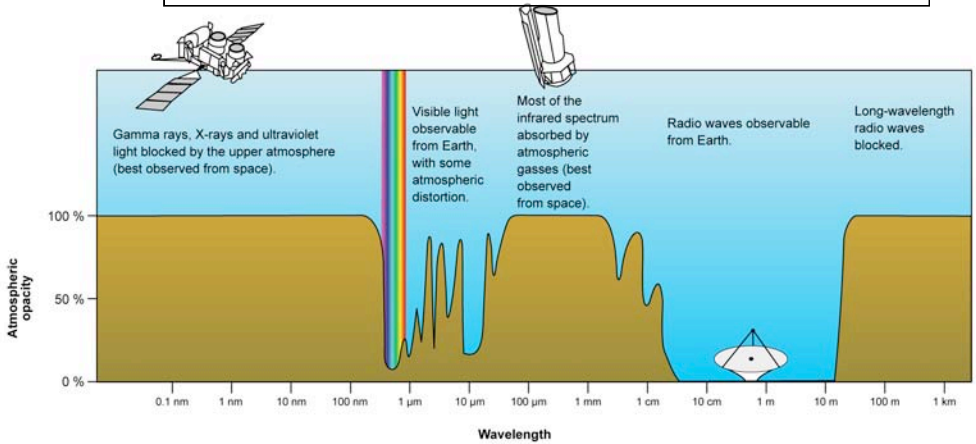

Different molecules absorb different wavelengths of radiation:

- O_2 and O_3 absorb almost all wavelengths shorter than 300 nm.
- Water (H_2O) absorbs many wavelengths above 700 nm, but this depends on the amount of water vapor in the atmosphere (tropics vs poles)
- When you combine the absorption spectra of the gasses in the atmosphere, you are left with "windows" of low opacity, allowing the transmission of only certain EMR.

Absorption of the Sun's incident electromagnetic energy in the Region from 0.1 to 30 mm by various atmospheric gases

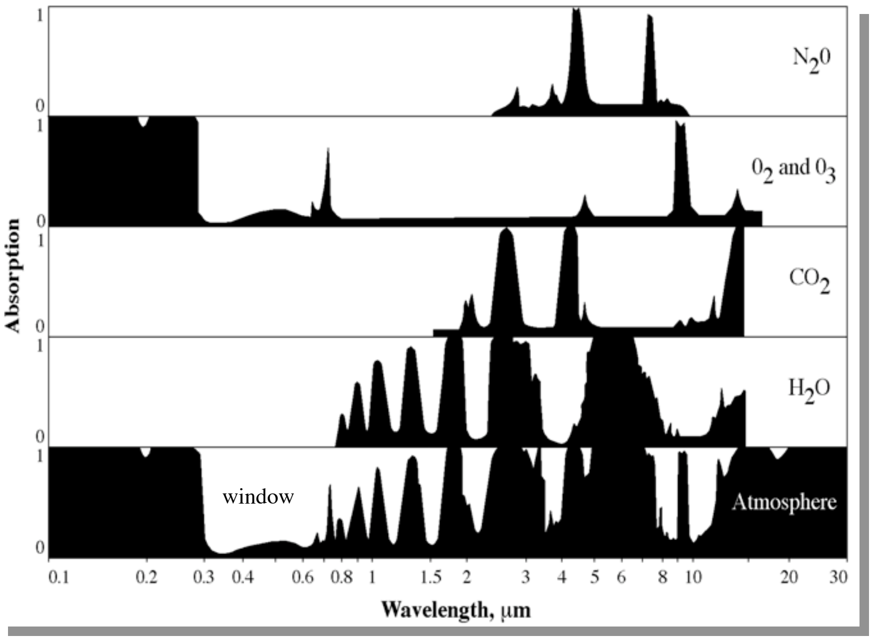

Jensen 2005

Interactions under consideration

- Interaction of EMR with the atmosphere

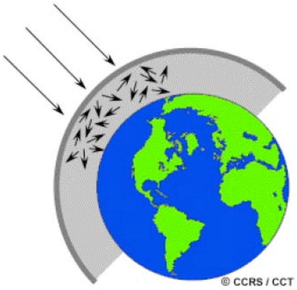

- Interaction of EMR with matter

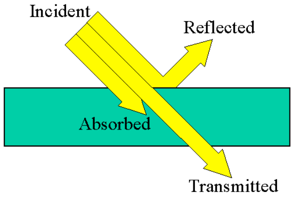

Interaction of EMR with matter

Radiative properties of natural surfaces

- Radiation incident upon a surface must either be *transmitted* (τ) through it, *reflected* (α) from the surface, or be *absorbed* (ξ).
- For solar radiation α is referred to as the surface *albedo*
- If we consider only part of the EM spectrum α is referred to as spectral reflectance

Transmissivity (τ) + Reflectivity (α) + Absorptivity (ξ) = 1

Radiative contribution in remote sensing

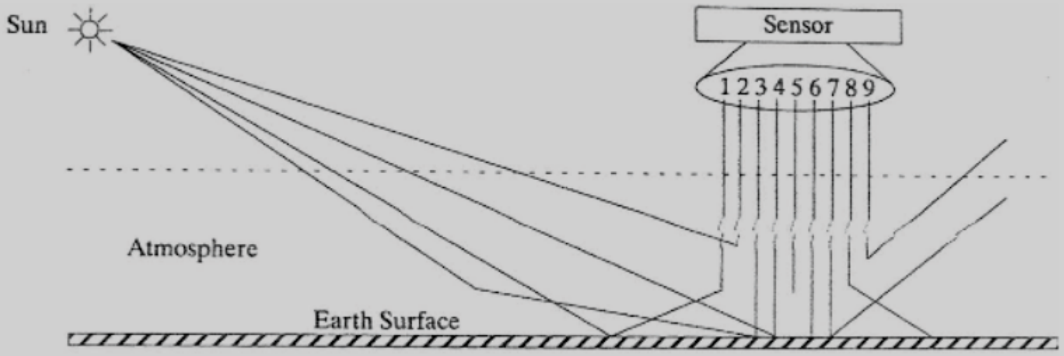

All first-order (direct) and second-order (single-scatter) radiance components are identified.

1. Sunlight scattered by atmosphere into sensor FOV
2. Adjacent ground radiance scattered into sensor FOV
3. Atmospheric emission reflected into sensor FOV
4. Sunlight reflected into sensor FOV
5. Direct atmospheric emission
6. Direct ground emission
7. Atmospheric emission reflected by ground
8. Ground emission scattered into sensor FOV
9. Atmospheric emission scattered into sensor FOV

FOV: field of view

Dispersion

Page 41-43 Rees

- When the dielectric properties (and therefore refractive index) of a medium vary with frequency, medium is said to be *dispersive*.

- Wave propagating through such media is called a *dispersive wave*.

- Wave or phase velocity given by $v = \frac{\omega}{k}$

  where ω is angular frequency and k is the wave number

- This is the speed at which the crests and roughs of the wave move in the propagation direction

- Group velocity $v_g = \frac{d\omega}{dk}$

Refraction

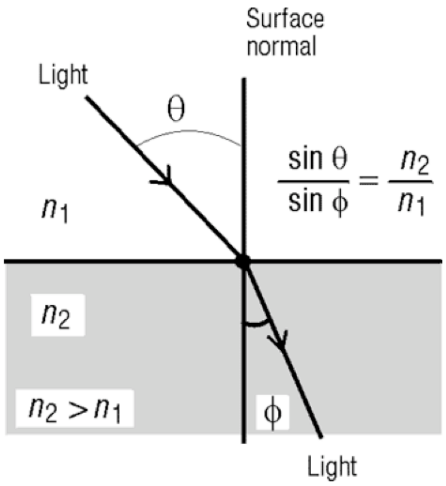

- When EMR passes from one medium to another, it changes direction (bends) at the interface because of the difference in speed of the wave in the media.
- Ratio of this speed difference is called the refractive index (n).
- Ratio of the refractive indices and the direction of the two rays of light for the two media are expressed in Snell's law:

$$\frac{n_2}{n_1} = \frac{\sin\theta}{\sin\phi}$$

where n1 and n2 are the refractive indices of the two media
θ is the angle of incidence
φ is the angle of refraction.

Complex dielectric constant

For most medium we shall need to consider, $\mu_r = 1$ (non magnetic materials)

If the medium absorbs energy from the wave, the dielectric constant becomes complex (real + imaginery)

$\varepsilon_r = \varepsilon' - i\varepsilon''$ or $\varepsilon_r = \varepsilon'(1 - \tan\delta)$

loss tangent

See page 36 of Rees, arrive at the following wave equation:

➔ $E_x = E_o \exp(-\omega kz/c) \exp(i [\omega t - \omega mz/c])$

Simple harmonic wave whose amplitude decreases exponentially with z
Flux density $F = F_0 \exp(-2\ \omega kz/c)$

➔ Absorption length $l_a = c/2\omega k$

Dielectric Properties of Materials

Rees discusses 4 categories of materials based on properties of their dielectric constant:

1) non-polar material ε' and ε'' are constant with ω.

2) polar material (water) ε' and ε'' vary with ω following the Debye equation.

3) conductive (salt water, copper) $\varepsilon'' = \dfrac{\sigma}{\varepsilon_0 \omega}$

4) plasma (ionosphere) $\varepsilon = n^2 = 1 - \dfrac{Ne^2}{\varepsilon_o m \omega^2}$

N - electron density

n -

m - electron mass

e - electron charge

For a plasma if $n > 0$ the waves are slowed as they travel through the ionosphere. If $n < 0$, n is purely imaginary and all the energy is reflected off the ionosphere. Under typical ionospheric conditions, low-frequency radio waves reflect while higher frequency microwaves can propagate through. Since the ionosphere is dispersive (i.e. speed depends on ω) a dual frequency microwave instrument (a radar altimeter or GPS) can measure the total electron content of a column of ionosphere and can use this to correct for the delay along the path of one or both frequencies.

Interaction of EMR with matter

Transmission

- Incident radiation passes through matter without attenuation
- Change of EMR is given by index of refraction n=n1/ n2 =sin θ 1/sin θ 2

Reflection (specular reflection)

- Surface is smooth relative to wavelengths
- Mirror-like surfaces are called specular reflectors

Scattering (diffuse reflection)

- Surface rough relative to wavelengths
- EMR velocity and wavelength are not affected but EMR is redirected

Absorption

- Substance is opaque to the incident radiation
- Portion of EMR is converted to heat energy (re-radiated)

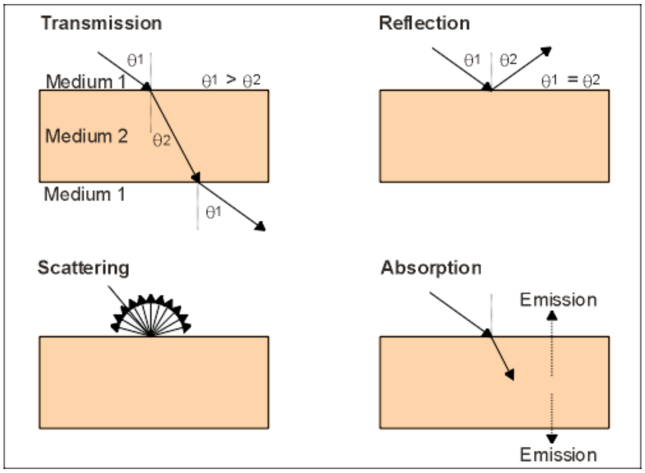

Interaction of EMR with matter

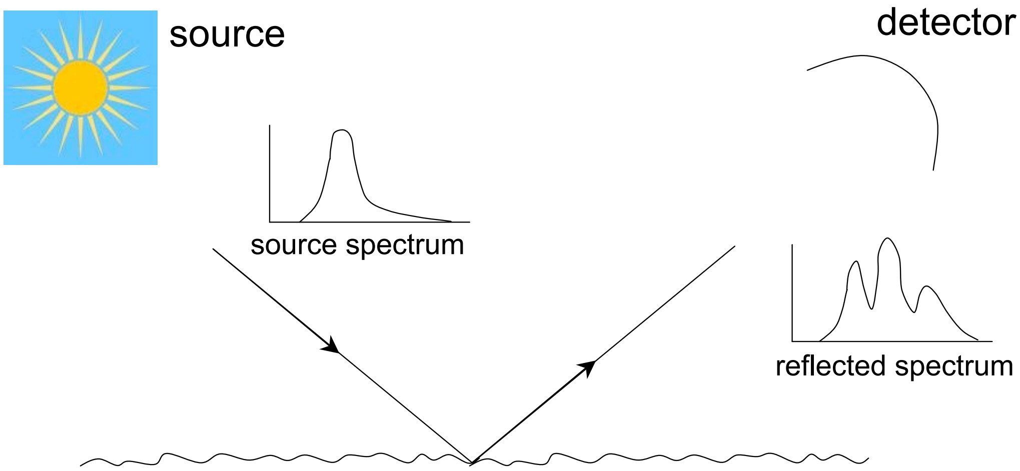

- Surface spectral imprint is embedded in the spectrum of the reflected wave
- Some incident energy is reflected and some is absorbed

Reflection from rough surfaces

- All active remote sensing systems as well as passive systems which measure reflected sunlight involve reflection of radiation from a rough surface
- Surface roughness is important even for passive systems which measure thermal emissions since r = 1 - ε
- Recall we have defined terms such as radiance and irradiance

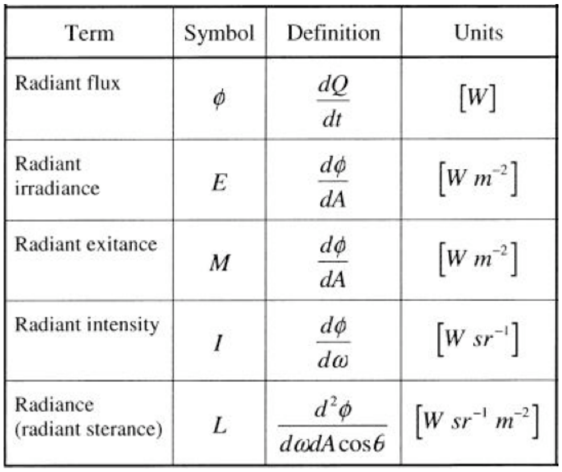

Term	Symbol	Definition	Units
Radiant flux	ϕ	$\frac{dQ}{dt}$	$[W]$
Radiant irradiance	E	$\frac{d\phi}{dA}$	$[W\ m^{-2}]$
Radiant exitance	M	$\frac{d\phi}{dA}$	$[W\ m^{-2}]$
Radiant intensity	I	$\frac{d\phi}{d\omega}$	$[W\ sr^{-1}]$
Radiance (radiant sterance)	L	$\frac{d^2\phi}{d\omega dA\cos\theta}$	$[W\ sr^{-1}\ m^{-2}]$

Radiance

Radiance (L_λ) is the radiant flux per unit solid angle leaving an extended source in a given direction per unit projected source area in that direction and is measured in watts per meter squared per steradian
($W\ m^{-2}\ sr^{-1}$).

We are interested in the radiant flux in certain wavelengths (L_λ) leaving the projected source area (A) within a certain direction (θ) and solid angle (Ω):

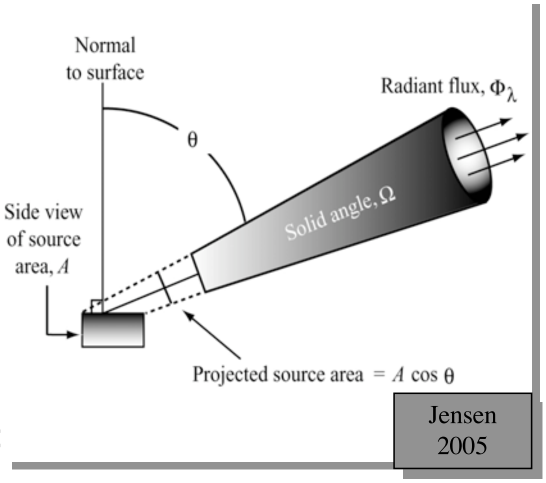

Jensen 2005

$$L_\lambda = \frac{\dfrac{\Phi}{\Omega}}{A\cos\theta}$$

units $W\ sr^{-1}\ m^{-3}$

Radiance

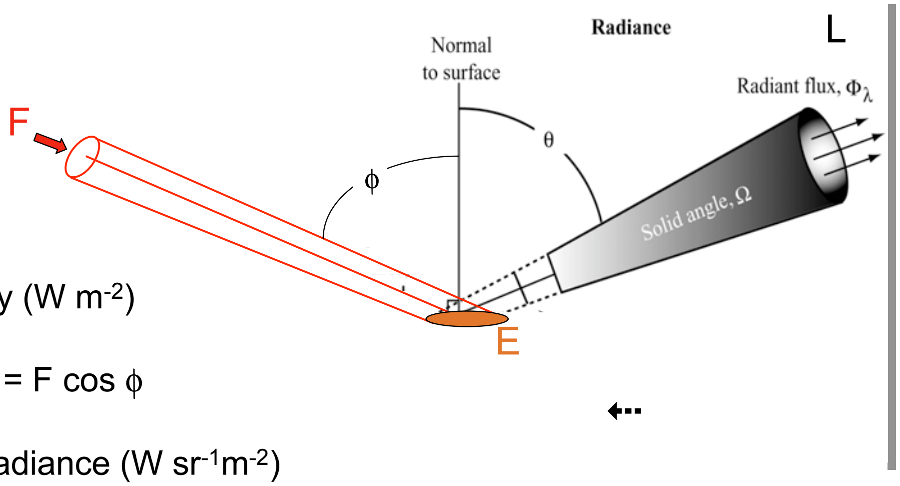

F - flux density ($W\ m^{-2}$)

E - irradiance = F cos ϕ

L - outgoing radiance ($W\ sr^{-1} m^{-2}$)

Assume there is no azimuthal dependence to reflected radiation

Surface scattering

1) Specular

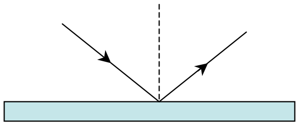

2) Quasi-specular

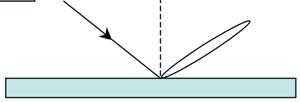

3) Lambertian

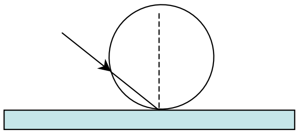

4) Minnaert model

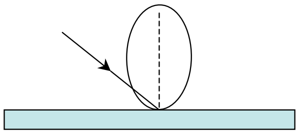

5) Henyey-Greenstein model for forward scatter

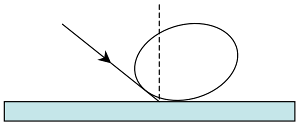

6) Henyey-Greenstein of backscatter

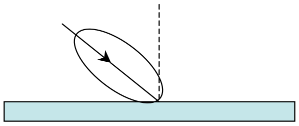

Bidirectional reflectance distribution function

$$r = \frac{L}{E} = \frac{\text{outgoing radiance}}{\text{irradiance}} \quad \text{sr}^{-1}$$

The reflectivity (or albedo, for light) of the surface is the ratio of:

$$\frac{\text{total power reflected}}{\text{total power incident}}$$

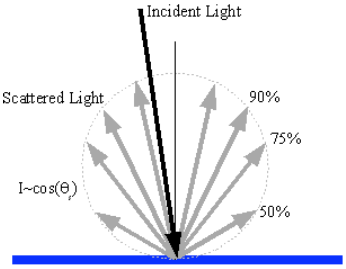

$$r(\phi) = \int_0^{2\pi} r(\theta)\, d\Omega$$

r can depend on the incidence angle ϕ

If we vary ϕ over all possible angles and average r we get the diffuse albedo:

$$r_d = \int_0^{2\pi} r(\phi)\, d\Omega \;\; / \, 2\pi$$

Reflectivity vs reflectance

- Reflectivity measures the fractional amplitude of the reflected electromagnetic field, while reflectance refers to the fraction of incident electromagnetic power that is reflected at an interface.

- Reflectance is the square of the magnitude of the reflectivity.

- The reflectivity can be expressed as a complex number, whereas the reflectance is always a positive real number.

Some typical albedos

Material	Albedo (%)	Albedo (0 to 1)
Water (naturally occurring)	1-10	0.01 to 0.1
Water (pure)	2	0.02
Forest	5-10	0.05-0.1
Crops	5-15	0.05-0.15
Urban areas	5-20	0.05-0.2
Grass	5-30	0.05-0.3
Soil	5-30	0.05-0.3
Cloud (low)	5-65	0.05-0.65
Lava	15-20	0.15-0.2
Sand	20-40	0.2-0.4
Ice	25-40	0.25-0.4
Granite	30-35	0.3-0.35
Cloud (high)	30-85	0.3-0.85
Limestone	35-40	0.35-0.4
Snow (old)	45-70	0.45-0.7
Snow(fresh)	75-90	0.75-0.9
Global average	~35	~0.35

Some typical albedos

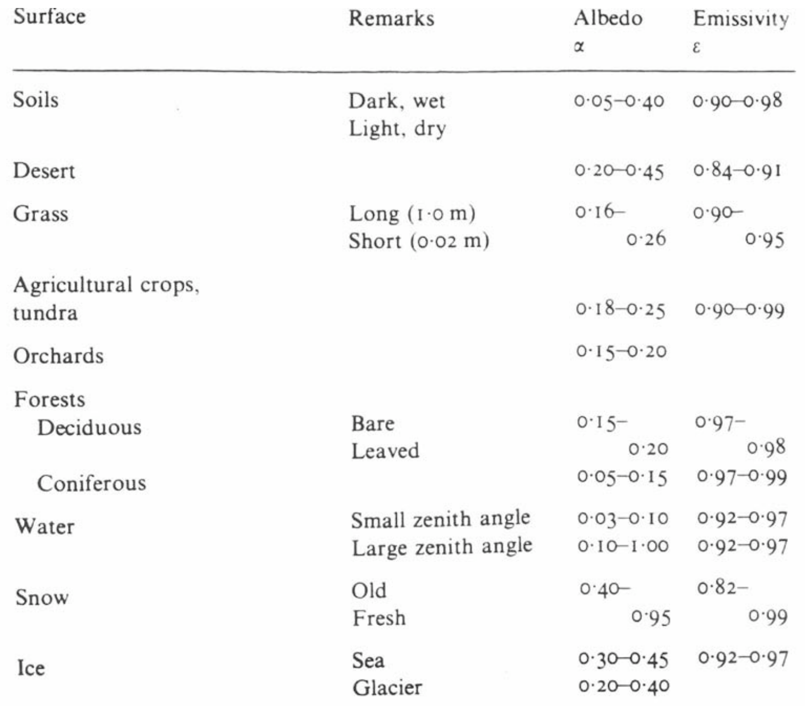

Surface	Remarks	Albedo α	Emissivity ε
Soils	Dark, wet Light, dry	0·05–0·40	0·90–0·98
Desert		0·20–0·45	0·84–0·91
Grass	Long (1·0 m) Short (0·02 m)	0·16– 0·26	0·90– 0·95
Agricultural crops, tundra		0·18–0·25	0·90–0·99
Orchards		0·15–0·20	
Forests			
Deciduous	Bare Leaved	0·15– 0·20	0·97– 0·98
Coniferous		0·05–0·15	0·97–0·99
Water	Small zenith angle	0·03–0·10	0·92–0·97
	Large zenith angle	0·10–1·00	0·92–0·97
Snow	Old Fresh	0·40– 0·95	0·82– 0·99
Ice	Sea	0·30–0·45	0·92–0·97
	Glacier	0·20–0·40	

Rayleigh criterion

The Rayleigh criterion is used to discriminate between smooth and rough surfaces.

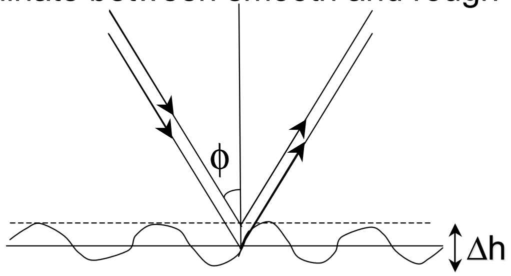

Δpath length $= 2\,\Delta h \cos\phi$

Phase difference $= \dfrac{2\pi}{\lambda}\, 2\,\Delta h \cos\phi$

Surface is considered smooth if phase difference < $\pi/2$

$\dfrac{4\pi\Delta h\cos\phi}{\lambda} < \pi/2$ or $\Delta h < \dfrac{\lambda}{8\cos\phi}$

For ordinary incidence angles $\Delta h < \lambda/8$

For 0.5 μm (blue light) $\Delta h < 62$ nm

For 8 cm (microwave) $\Delta h <$ 1 cm

Surface roughness in radar imagery

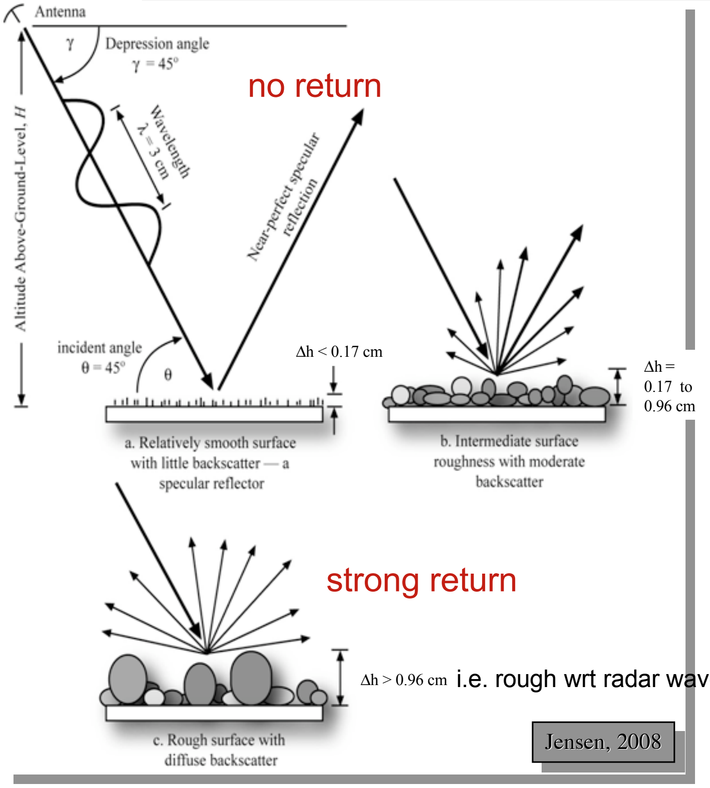

Expected surface roughness back-scatter from terrain illuminated with 3 cm wavelength microwave energy with a depression angle of 45˚.

Radar backscatter

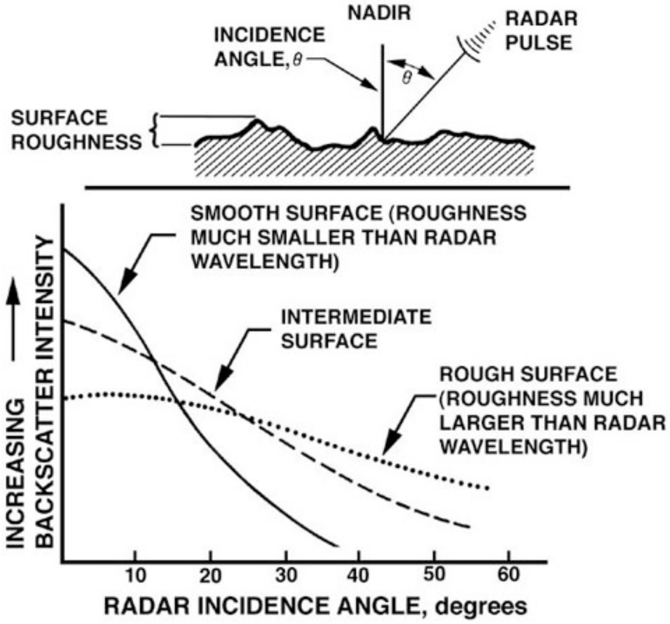

For angles less than about 25º smoother surfaces have higher backscatter than rougher surfaces

Surface Roughness

- Surface roughness is the terrain property that most strongly influences the strength of the EMR backscatter.

- In radar imagery surface roughness characteristics are micro-relief rather than topographic relief (as with visible imagery)

- There is a relationship between the wavelength of the radar (λ), the depression angle (θ), and the local height of objects (h in cm) found within the resolution cell being illuminated by EMR. It is called the modified Rayleigh criteria and can be used to predict what the earth's surface will look like in a radar image if we know the surface roughness characteristics and the radar system parameters (λ,g ,h) mentioned.

Backscattering coefficients

Typical values of the dimensionless backscattering coefficient σ^0, as a function of incident angle

(*a*) X-band; (*b*) Ku-band.

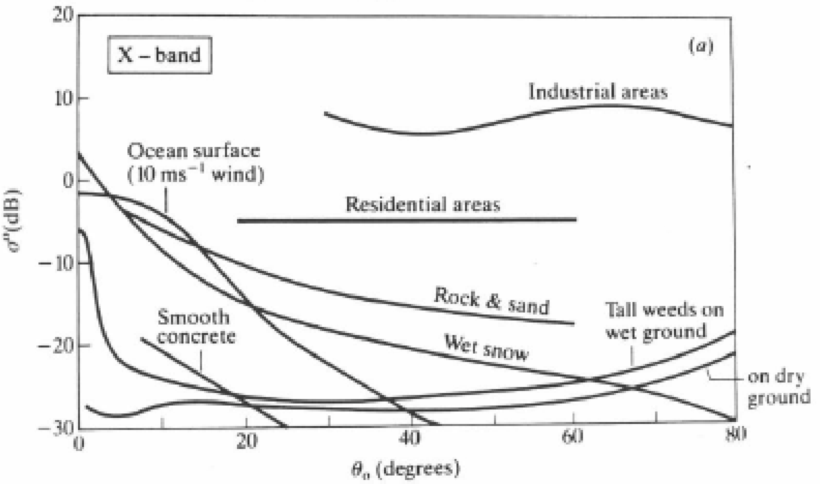

Surface melting in Greenland

Image from optical sensor AVNIR-2 on July 3, 2008 (day)

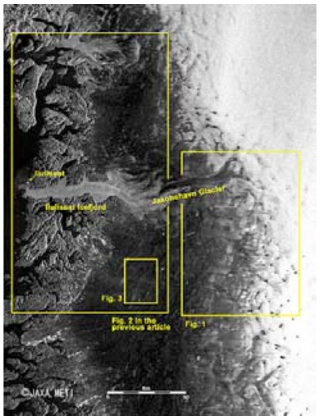

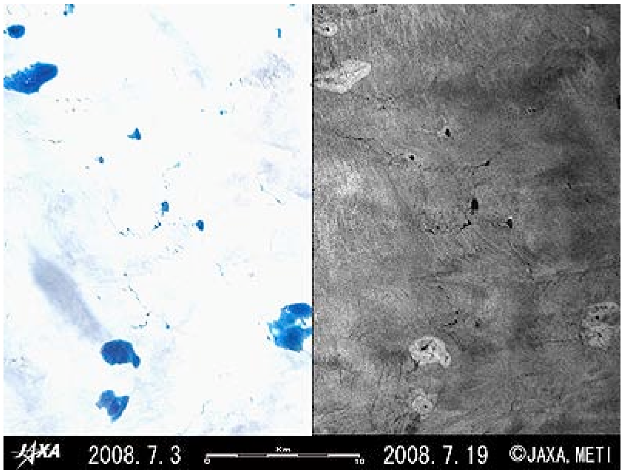

Image from PALSAR two weeks later (night).

Melt ponds appear blue in the left image and are either black or brighter than the surroundings in the right image.

Black: very little of PALSAR's radar signal is returned to the satellite, indicating that the surface is smooth, unfrozen water.

Bright gray: some of PALSAR's radar signal returns to the satellite, suggesting that the frozen surface contains many air bubbles or that the water surface is ruffled but unfrozen.

Surface melting in Greenland

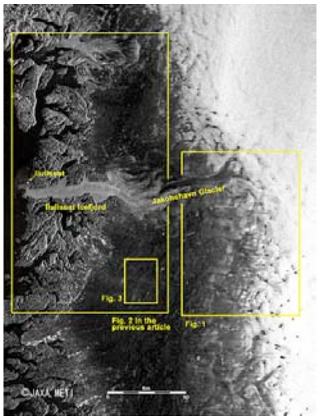

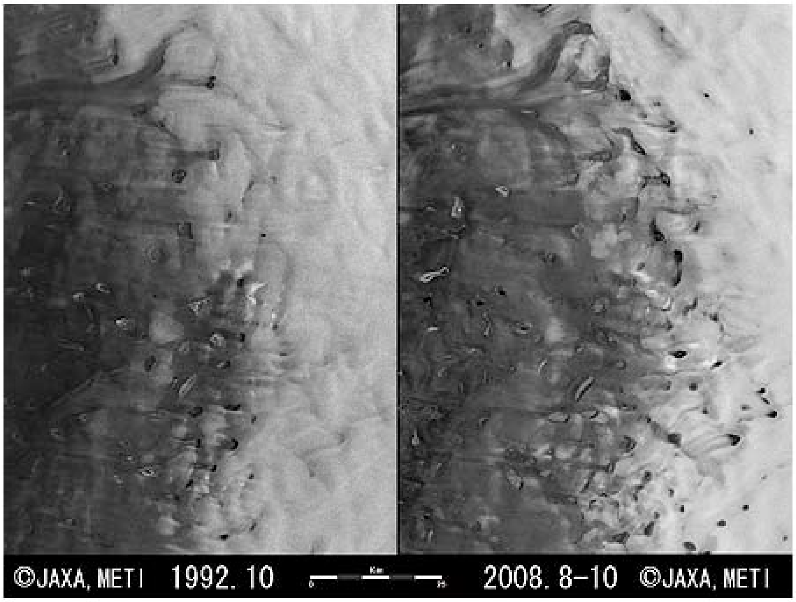

Fig. 1 Changes of melt ponds on ice sheet in western Greenland in last 16 years

SAR images of 100 to 175km area in western Greenland. The left image acquired by JERS-1 in October 1992; right image acquired by ALOS August and in October of 2008.

Surface melting in Antarctica

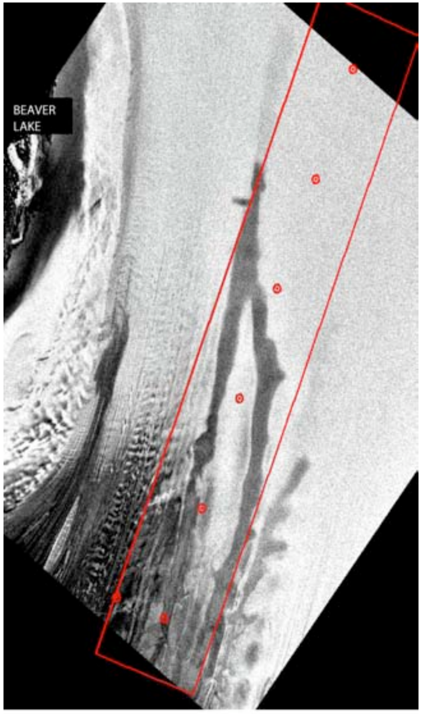

SAR image acquired over Amery Ice Shelf survey region on 15 August 1993.

Dark wish-bone shaped feature is a surface meltstream, only active during austral summer

Bragg scattering

Page 53-55 Rees

- Consider a surface where z(x) << λ. The surface is smooth so most of the incident energy undergoes specular reflection.
- For an active system such as SAR, most of the energy will not return to the radar.
- However, if the rough surface has a characteristic λ that matched the radar wavelength, then one can get resonant scattering
- This commonly occurs over the ocean and is called Bragg scattering (just like the scattering of light from regular crystal lattices).

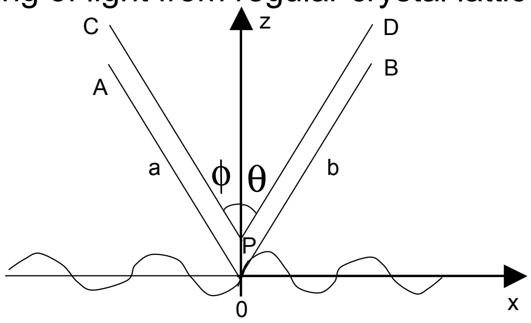

What is the phase difference between paths AB and CD?

Bragg scattering

Page 53-55 Rees

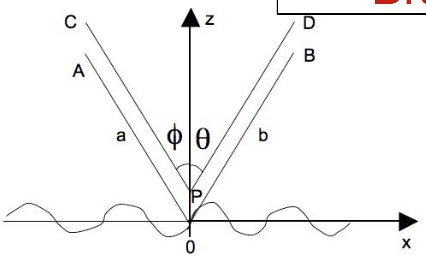

AO = a and OB = b

CP = a + x sin φ - z(x) cos φ

PD = b - x sin θ - z(x) cos θ

$$\text{path difference } \Delta s = a - b = x\underbrace{(\sin\phi - \sin\theta)}_{\alpha} - z(x)\underbrace{(\cos\phi - \cos\theta)}_{\beta}$$

$$\text{phase difference } \Delta\phi = 2\pi/\lambda\,\Delta s = k\,\Delta s = k\,(\alpha x - \beta z)$$

The total amplitude scattered from direction φ into direction θ is:

$$E = \int_{-\infty}^{\infty} e^{-i\phi(x)}\,dx = \int_{-\infty}^{\infty} e^{-ik\alpha x}\,e^{ik\beta z(x)}\,dx$$

$E = \Im\,[\,e^{ik\beta z(x)}]$ but z(x) << λ so expand exponential in a Taylor series and lose higher power terms:

$$e^{ik\beta z(x)} = 1 + ik\beta z(x) - \cancel{\frac{(k\beta z)^2}{2!}} + \ldots \qquad E = \boxed{\int_{-\infty}^{\infty} e^{-ik\alpha x}\,dx} + ik\beta\int_{-\infty}^{\infty} z(x)\,e^{-ik\alpha x}\,dx$$

δ-function δ(kα) at α = 0 (which is the specular component φ = θ)

Bragg scattering

Page 53-55 Rees

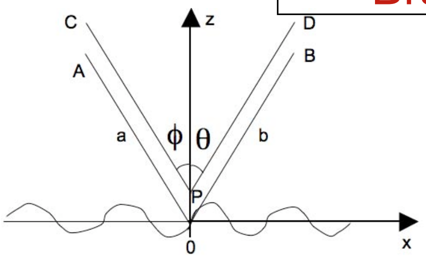

$$E = \boxed{\int_{-\infty}^{\infty} e^{-ik\alpha x}\,dx} + ik\beta\int_{-\infty}^{\infty} z(x)\,e^{-ik\alpha x}\,dx$$

δ-function δ(kα) at α = 0

$$\text{Let } z(x) = \int_{-\infty}^{\infty} z(q)\,e^{iqx}\,dq$$

$$\text{2nd term becomes } = ik\beta\int_{-\infty}^{\infty}\int_{-\infty}^{\infty} z(q)\;e^{-i(q-k\alpha)x}\,dq\,dx$$

$$= ik\beta\int_{-\infty}^{\infty} z(q)\underbrace{\boxed{\int_{-\infty}^{\infty} e^{-i(q-k\alpha)x}\,dx}}_{2\pi\,\delta(q-k\alpha)}\,dq$$

$$= 2\pi\,ik\beta\int_{-\infty}^{\infty} z(q)\,\delta(q-k\alpha)\,dq\,dx$$

This integral selects the topography with q = kα

Bragg scattering

Page 53-55 Rees

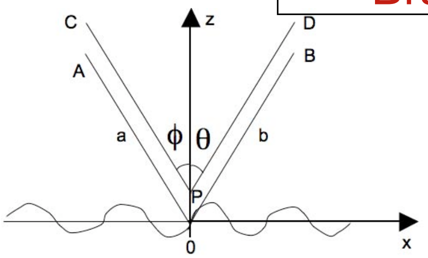

$$E = \boxed{\int_{-\infty} e^{-ik\alpha x}\, dx} + ik\beta \int_{-\infty}^{\infty} z(x)\, e^{-ik\alpha x}\, dx$$

δ-function $\delta(k\alpha)$ at $\alpha = 0$

Let $z(x) = \int_{-\infty}^{\infty} z(q)\, e^{iqx}\, dq$

2nd term becomes $= 2\pi\, ik\beta \int_{-\infty}^{\infty} z(q)\, \delta(q-k\alpha)\, dq\, dx$

This integral selects the topography with $q = k\alpha$

Let $\phi = -\theta$ for a single radar $\alpha = 2\sin\theta$

$$\frac{2\pi}{\lambda_s} = \frac{2\pi\, 2\sin\theta}{\lambda_r} \Rightarrow \boxed{\lambda_s = \frac{\lambda_r}{2\sin\theta}}$$

Bragg scattering

Page 53-55 Rees

- As the incidence angle of the ERS SAR is oblique (23°) to the local mean angle of the ocean surface, there is almost no direct specular reflection except at very high sea states.
- It is therefore assumed that at first approximation Bragg resonance is the primary mechanism for backscattering radar pulses.
- The Bragg equation defines the ocean wavelengths for Bragg scattering as a function of radar wavelength and incidence angle

$$\lambda_s = \frac{\lambda r}{2\sin\theta}$$

where λ_r radar wavelength
λ_s sea surface wavelength
θ incidence angle

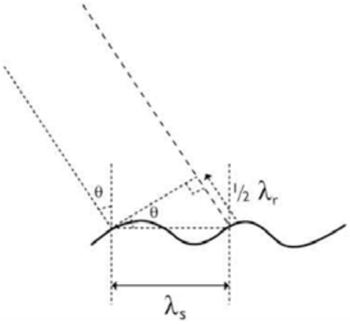

- The short Bragg-scale waves are formed in response to wind stress. If the sea surface is rippled by a light breeze with no long waves present, the radar backscatter is due to the component of the wave spectrum which resonates with the radar wavelength.

Radar imaging

- Radar does not detect the visible colour of the surface, but detects the moisture (or lack of it) and EM properties of the surface
- Radar systems record the phase and polarisation (orientation of EM) of the reflected pulse
- Radar produces images with speckle due to the coherent nature of the system
- Radar produces images with certain geometric distortions such as slant range geometry, image layer and shadowing

Subsurface penetration

For imaging radars, two types of penetration must be considered -- atmospheric and surface

- Only K_a-band (0.8-1.1cm) radar has some cloud mapping capability
- C-, L- and P-band radars are defined as “all weather”
- X-band radar does not penetrate heavy precipitation
- The depth of passive microwave penetration into a surface medium is strongly dependent upon wavelength and the complex dielectric constant (ε)
- With increasing λ, penetration increases
- With increasing ε, penetration decreases and reflectivity increases

SAR imaging (active microwave)

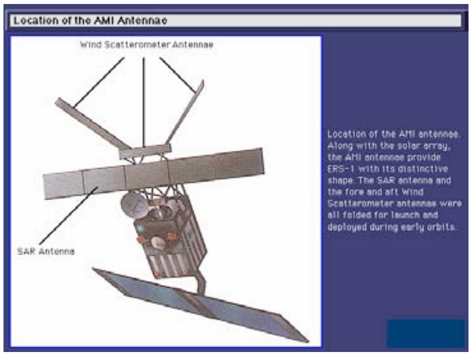

Location of the AMI antennae. Along with the solar array, the AMI antennae provide ERS-1 with its distinctive shape. The SAR antenna and the fore and aft Wind Scatterometer antennae were all folded for launch and deployed during early orbits.

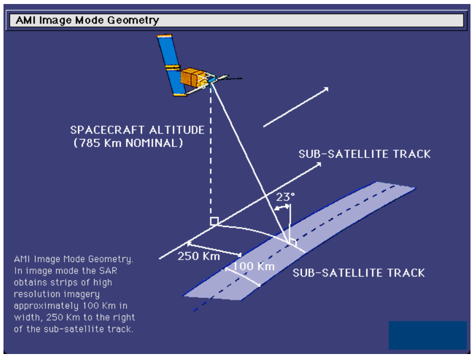

AMI Image Mode Geometry. In image mode the SAR obtains strips of high resolution imagery approximately 100 Km in width, 250 Km to the right of the sub-satellite track.

ERS Active Microwave Instrument (AMI) operates at 5.3 GHz (C-band) combines the functions of a Synthetic Aperture Radar (SAR) and a Wind Scatterometer (WNS). Four antennae (three for the Scatterometer and one for the SAR) illuminate Earth's surface -- backscattered energy is received to produce data on wind fields and wave spectra, and to prepare high resolution images

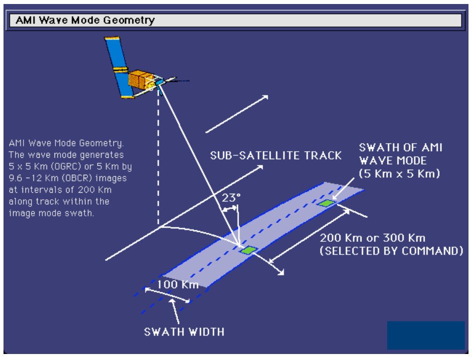

AMI Wave Mode Geometry. The wave mode generates 5 x 5 Km (OGRC) or 5 Km by 9.6 -12 Km (OBCR) images at intervals of 200 Km along track within the image mode swath.

Conditions for subsurface radar imaging

1. Cover material must be extremely dry (<1% moisture content)
2. Cover material must be fine-grained (r = 1/10λ)
3. Cover material must be free of clay minerals (water-bearing minerals)
4. Subsurface must be rough enough to generate backscatter

10% of the earth's surface is amenable to subsurface imaging

Imaging radars can penetrate vegetation canopies

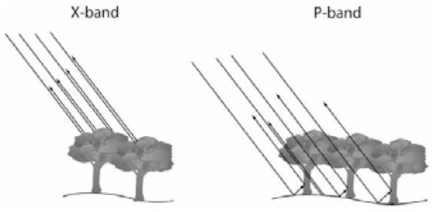

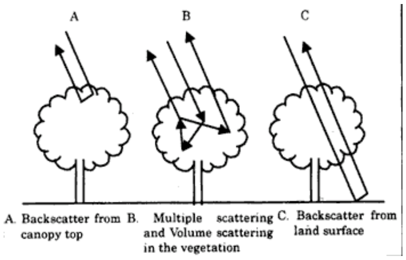

Conditions for subsurface radar imaging

Color composite image of southern Bahia, Brazil acquired by the SIR-C/X-band SAR on October 2, 1994.

The high resolution capability of SIR-C/X-SAR imaging and the sensitivity of its frequency and polarization channels to various land covers are used for monitoring and mapping areas of importance for conservation.

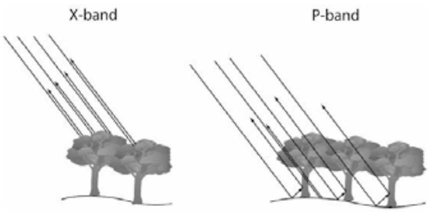

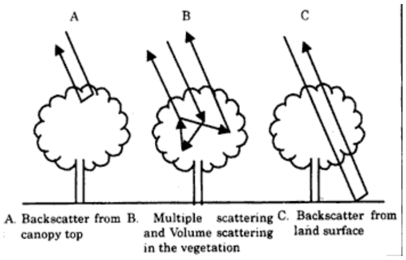

Submarine detection

- Vortices and internal waves generated by submarines modulate the wavelength of the short surface waves
- Short wave amplitude spectrum proportional to λ^4
- Bragg scattering dominates the ocean surface reflection for SAR incidence angles of 20-70°
- Surface convergence = radar bright
- At what radar wavelength are submarine wakes most visible? (many clear examples in Seasat data; 30 m resolution is adequate)

Ocean features from SAR

Mesoscale oceanic phenomena become visible on SAR images because they are associated with variable surface currents which modulate the surface roughness.

Internal waves in the Gibraltar Strait

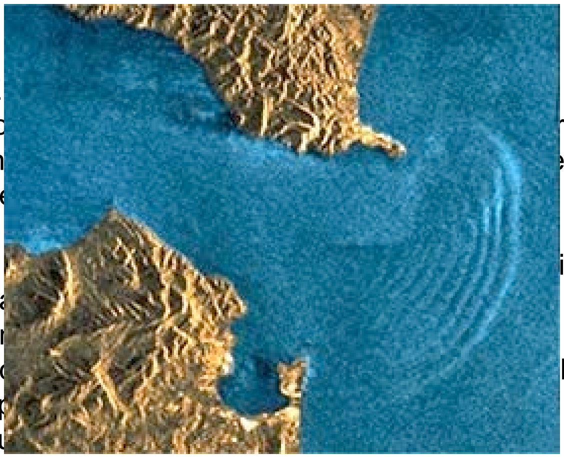

E which
ro r
in e
de

If ight
pa
ur
oc he
sp sea
su

Ocean features from SAR

Mesoscale oceanic phenomena become visible on SAR images because they are associated with variable surface currents which modulate the surface roughness.

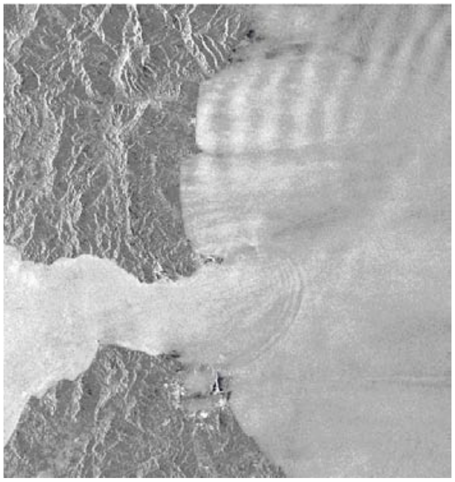

Internal waves in the Gibraltar Strait

ERS-1 SAR image of same area.

Shows in the center sea surface manifestations of an oceanic internal wave packet generated in the Strait of Gibraltar. In the lower right part of the image is possible to recognize surface manifestation of atmospheric internal waves (lee waves) generated by an eastward blowing wind over the 600 m high mountain range Sierra de Hauz in Morocco.

Ship wake detection by SAR

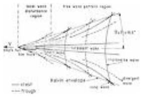

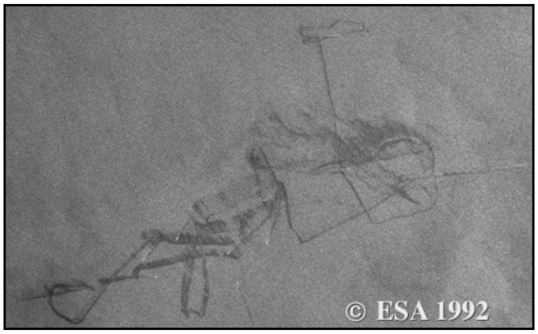
© ESA 1992

- A wide range of ship sizes may be detected under a variety of sea-state conditions. Radar can infer ship size, and if a wake is present, its speed and direction of travel.

- HH polarisation is less sensitive to wake detection.

- Potential users of this information include agencies who monitor ship traffic, authorities responsible for sovereignty and fisheries surveillance, as well as customs and excise agencies charged with stopping illegal smuggling activities.

Ship wake detection by SAR

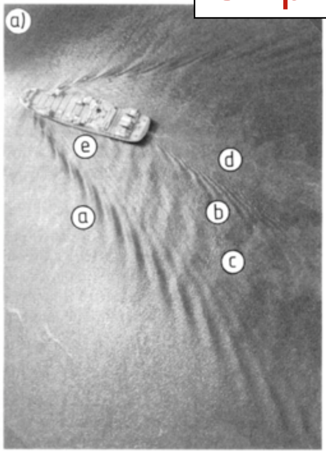

ith larger incidence angles, the ocean background
ter effects are reduced, increasing signal to noise.
ship is a bright point target against the ocean
kground clutter and can be detected using image
esholding techniques.
s the ocean clutter increases with increasing wind
eds, ship detection becomes more difficult. At wind
eds > 10 m/s it is difficult to detect small fishing
sels.
s the wind speeds increase, the radar cross-section
he ocean increases, reducing the contrast between
feature of interest and the surrounding ocean.

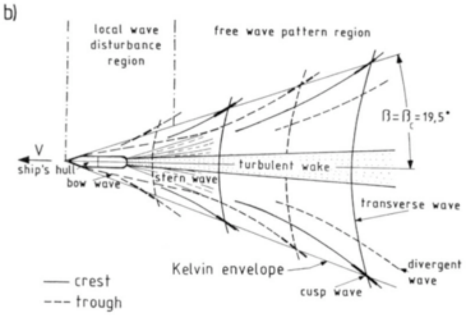

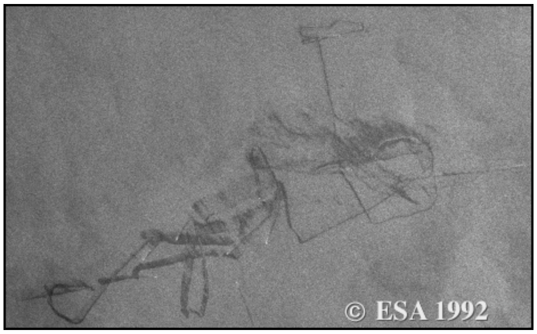
© ESA 1992

Oil spill detection by SAR

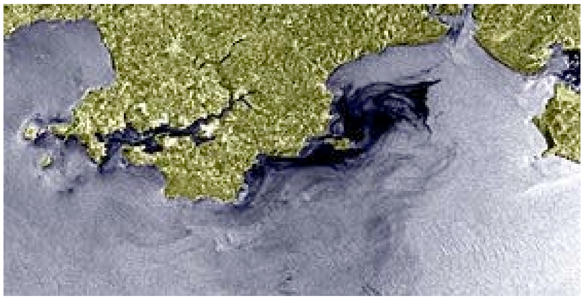

RADARSAT image of coastal oil spill, Wales (Courtesy CCRS)

- Oil slicks and natural surfactants are imaged through the localised suppression of Bragg scale waves.
- Oil spills also have a darker tone with respect to the surrounding ocean background.
- Detection of an oil spill is strongly dependent upon the wind speed. At wind speeds > 10 m/s, the slick will be broken up and dispersed, making it difficult to detect.
- Small incidence angles are optimum for oil spill detection.
- Detection will also depend on the spill size and image resolution.

Scatterometry

- Scatterometry is a form of radar remote sensing that can measure various geophysical properties of surfaces and volumes based on the amplitude of microwave electromagnetic pulses that are transmitted from and scattered back to an antenna aboard the spacecraft.

- Scatterometer is a radar system that provides a quantitative measure of the backscattering cross section as a function of the incident angle.

  - ➢Backscatter cross-section is a measure of how detectable an object is with a radar. When radar-waves are beamed at a target, a number of different factors determine how much electromagnetic energy returns to the source, such as the angles created by the surface/plane intersections.

- A scatterometer transmits a continuous signal or a series of pulses and the strength of the returned signal is recorded.

http://cires.colorado.edu/~maurerj/scatterometry/what_is_scatterometry.htm

Wind speed retrieval by scatterometer

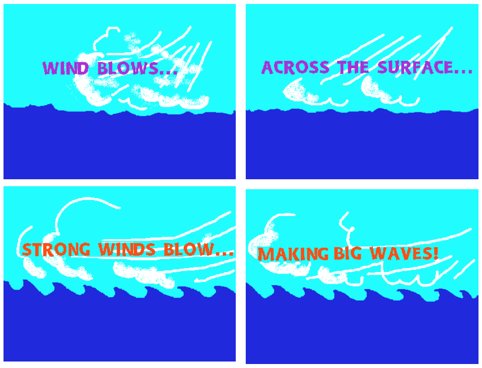

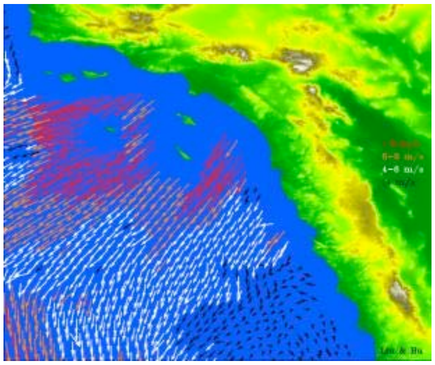

Santa Ana winds off CA coast

Example: SeaWinds scatterometer on QuikScat -- a microwave radar designed specifically to measure ocean near-surface wind speed and direction.

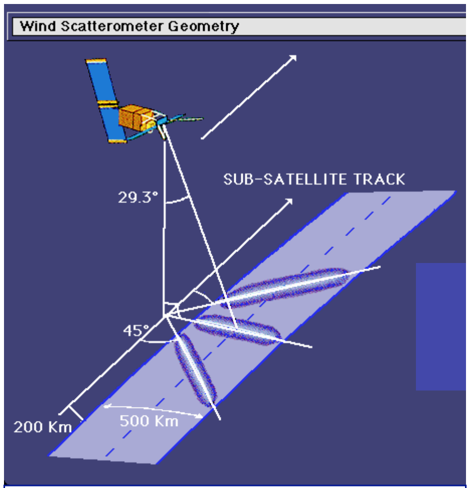

The three Wind Scatterometer antennae generate radar beams 45° forward, sideways and 45° backwards across a 500km wide swath, 200km to the right of the sub-satellite track.

Wind speed retrieval by scatterometer

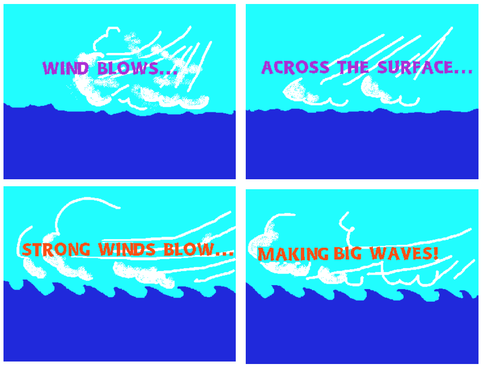

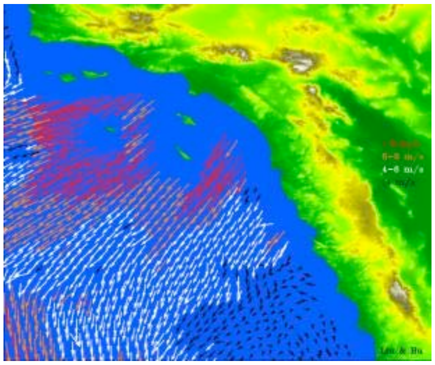

Santa Ana winds off CA coast

Example: SeaWinds scatterometer on QuikScat -- a microwave radar designed specifically to measure ocean near-surface wind speed and direction.

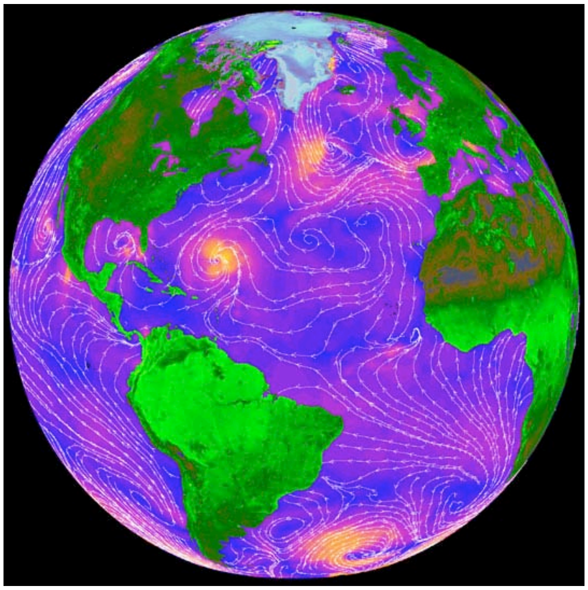

MISR mapping of surface roughness

Surface roughness at sastrugi scale has large effect on optical scattering

Megadunes field site, 2002

- Smooth surfaces are forward scattering; brighter when sun is in front of viewer

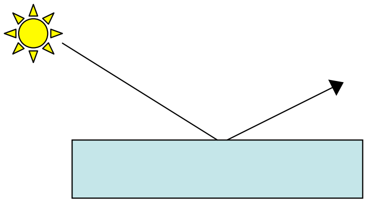

- Rougher surfaces are backscattering; brighter when sun is behind viewer

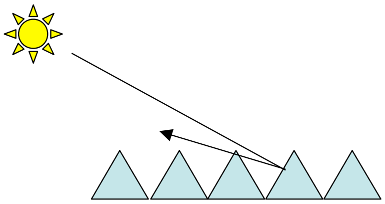

MISR (Multi-angle Imaging Spectro-Radiometer) can detect this effect and quantify it

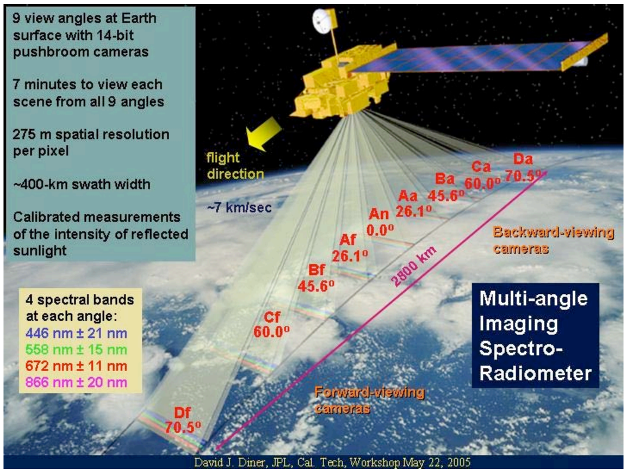

9 view angles at Earth surface with 14-bit pushbroom cameras

7 minutes to view each scene from all 9 angles

275 m spatial resolution per pixel

~400-km swath width

Calibrated measurements of the intensity of reflected sunlight

4 spectral bands at each angle:
446 nm ± 21 nm
558 nm ± 15 nm
672 nm ± 11 nm
866 nm ± 20 nm

Multi-angle Imaging Spectro-Radiometer

David J. Diner, JPL, Cal. Tech, Workshop May 22, 2005

Flies on the NASA Terra platform (w/ MODIS, ASTER);

275 m resolution; 380 km swath;

Latitude limit: ~82.8° S

DESCRIPTION OF THE MISR INSTRUMENT

Camera Angles	±70.5°, ±60.0°, ±45.6°, ±26.1°, 0°
Spectral Bands	448 nm (Blue), 558 nm (Green), 672 nm (Red), 866 nm (near IR)
Pixel Size	275 × 275 m (all bands in nadir camera and red bands in all other cameras) 1.1× 1.1 km (blue, green, and near-IR bands in fore and aft cameras)
Swath Width	380 km

Our algorithm:

- **red channel (275m)**
- **±60° view fore/aft (Cf and Ca ‘cameras’)**
- **normalized difference ratio:**

$$\frac{Cf - Ca}{Cf + Ca}$$

MOA Optical Snow Grain Size Mapping

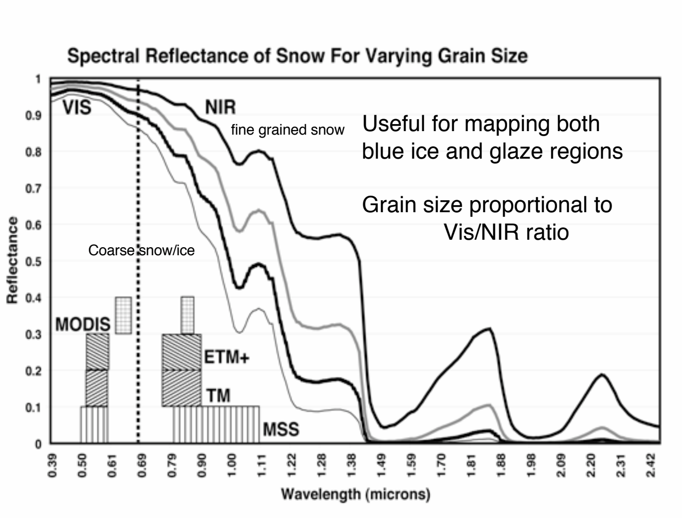

Useful for mapping both blue ice and glaze regions

Grain size proportional to Vis/NIR ratio

- uses band 1 (red) and band 2 (infrared)
- atm. and BRDF correction provided by SBDART
- validation from snow refl. spectra on sea ice in October 2003